Radiometry performance of the VGOS receivers of the Onsala twin telescopes

Radiometry performance of the VGOS receivers of the Onsala twin telescopes

G. Elgered, P. Forkman, R. Haas, E. Varenius

Abstract We have assessed to stability of the present VGOS receivers in the Onsala twin telescopes (OTT) in order evaluate the possibility to use them to estimate the wet propagation delay of the atmosphere. As expected the highest possible frequencies that can be used in the present OTT receivers, 15.3 to 15.6 GHz, are too far from the centre of the water vapour emission line at 22.2 GHz in order to be meaningful for critical assessments of the wet delays estimated from the VLBI data themselves. However, we do find clear correlations between the wet delays estimated from the VGOS receivers with those provided by a traditional stand-alone microwave radiometer.

Keywords microwave radiometry, VGOS, wet delay

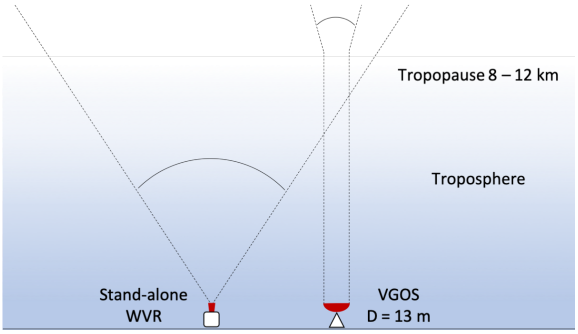

Fig. 1 The geometry of the sensed atmosphere. The typical dimension of the feed of the stand-alone WVR implies that almost all water vapour will be present in the far field of the antenna pattern (Balanis, 2005). On the other hand, for the VLBI telescope and elevation angles above 15° most of the water vapour is in the near field (from Forkman et al., 2021).

1 Introduction

An important difference when using a stand-alone water vapour radiometer (WVR) for calibration, or assessment, of the wet propagation delays estimated from geodesy VLBI data is the different air masses sampled by the telescope and the WVR (see Fig. 1). Petrachenko et al. (2009) suggested to use VGOS receivers also as a radiometers to observe the sky emission simultaneously with the VLBI source, provided that the observed frequency was close enough to the water vapour emission line at 22.2 GHz.

A simulation was performed by Forkman et al. (2021) in order to study the accuracy of the estimated wet delay. The simplest approach is to use one frequency only, to be used when no liquid water is present in the atmosphere. Fig. 2 summarise these results, presented as the expected standard deviation (SD) for three different levels of white noise of the observed sky temperature.

When clouds containing liquid water are present, there is a need to observe the sky emission at two different frequencies, with different emission properties due to water vapour and liquid water. That means two observations and two unknowns, the wet delay and the liquid water content in the direction of the observation. The concept that has been used since several decades is to have one frequency close to the water vapour emission line and one frequency around 31 GHz (Wu, 1979). In the work by Forkman et al. (2021) the range of frequencies were, however, restricted to the 14–24 GHz interval, assuming that a similar range

Gunnar Elgered, Peter Forkman, Rüdiger Haas, Eskil Varenius
Chalmers University of Technology, Onsala Space Observatory, SE-439 92 Onsala, Sweden

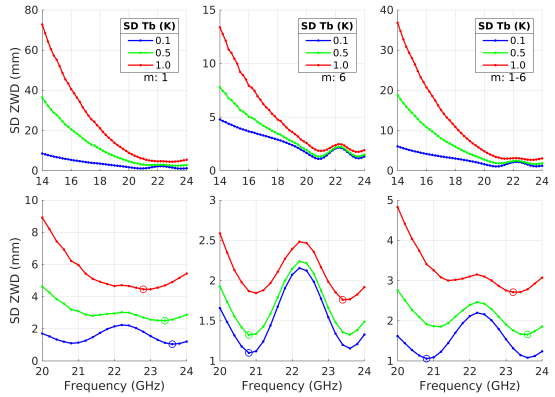

Fig. 2 The expected accuracy in the equivalent zenith wet delay (ZWD). Left: 1 airmass, middle: 6 airmasses, and right: 1–6 airmasses. The lower plots zoom in on the frequency range giving the lowest standard deviation (SD). The circles mark the lowest SD at the optimal frequency (from Forkman et al., 2021).

could be used in a future generation of VGOS receivers. The corresponding simulated results are presented in Fig. 3.

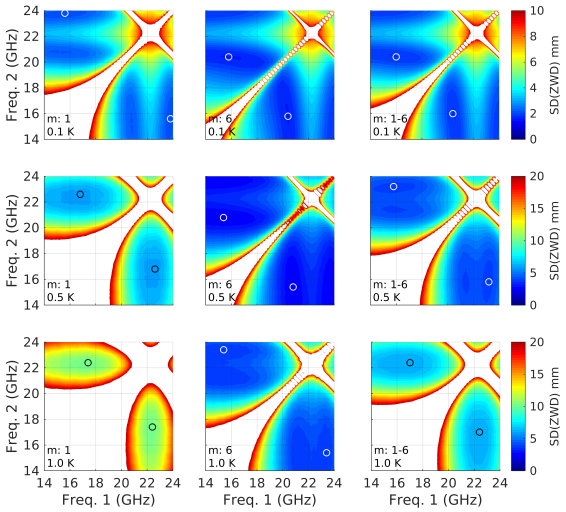

Fig. 3 The expected ZWD rms error (SD) for a two-frequency algorithm (one frequency at each axis in the graphs) for 1 (left), 6 (middle) and 1–6 (right) airmasses. The receiver noise is simulated as 0.1 K (top), 0.5 K (middle), and 1.0 K (bottom) for each row. The white areas correspond to rms errors larger than the upper limit of the scale and the circles mark the lowest rms error obtained for the optimal frequency pair (from Forkman et al., 2021).

2 Observations

The Onsala twin telescopes are equipped with different receivers. The northeast telescope (OE) has a QRFH feed and the southwest telescope (OW) has an Eleven feed (see Fig. 4). Fig. 5 depicts the receiver noise temperatures measured using the Y-factor method. For more details on the OTT receivers see Pantaleev et al. (2017).

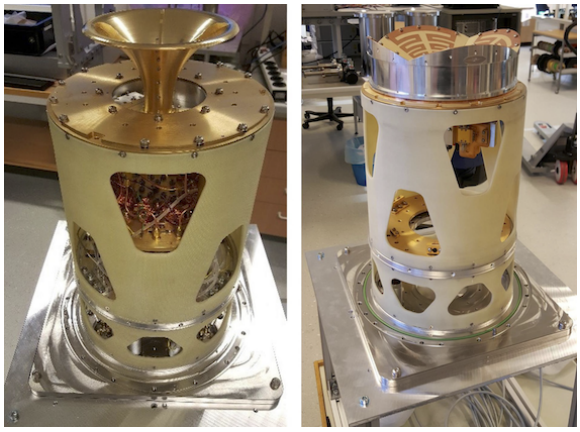

Fig. 4 Receivers in the Onsala twin telescopes. The receiver with the QRFH feed is in the OE telescope (left) and the receiver with the Eleven feed is in the OW telescope (right) (from Pantaleev et al., 2017).

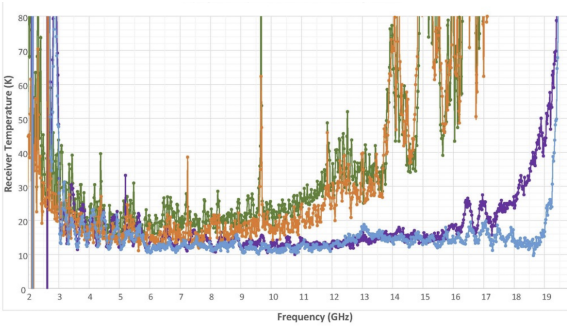

Fig. 5 Lab measurements of the receiver temperatures for the two different polarizations (vertical and horizontal), OE: blue/purple and OW: orange/green (from Pantaleev et al., 2017).

2.1 OTT radiometric data sets

Because our approach was to use radiometry data from the VGOS receivers in one frequency band only, the observations had to be acquired during periods with no liquid water in the atmosphere. This together with the fact that OTT also were scheduled to carry out regular geodesy VLBI observations during the winter-spring period of 2023, resulted in two measurement campaigns:

- OW was used from 28 February to 2 March 2023. Elevation angles: 8°, 20°, and 90°.
- OE was used from 8 to 12 May 2023. Elevation angles: 10°, 20°, and 90°.

During both periods the azimuth angle of the OTT was 220°, where the horizon is defined by the sea surface, in order to minimise the ground noise pickup.

2.2 OTT measurement sequence

The system temperature was measured every 1 s for 1 min at the three different elevation angles. Measurements were carried out in 8 frequency bands, 32 MHz wide, from 15,344 to 15,600 GHz, and for both horizontal and vertical polarizations. The mean value was calculated for each channel for every 1 min period. Because of intermittent interference the value was ignored if the SD was > 1 K (1.5 K at the lowest elevation angle to allow for more atmospheric variability). Thereafter, the mean value of all 16 channels was calculated, and for every 3 min period a tip curve analysis and the method of least squares was used to estimate the equivalent zenith sky brightness temperature due to the atmosphere, including the cosmic background radiation of 2.7 K, and the receiver temperature, assuming a horizontally homogeneous atmosphere.

2.3 Stand-alone WVR Konrad

In order to assess the quality of the estimated sky brightness temperatures and the ZWD from the VGOS receivers, we used the 20.64 GHz channel of the Konrad WVR. The second channel, usually utilized for correction of liquid water in the atmosphere, was not used, because both data sets were acquired during conditions without liquid water clouds. Konrad was scanning the sky in 17 different directions (varying both the azimuth and the elevation angles) in a repeating duty cycle of approximately 2 min. For more details on the Konrad WVR observations and the corresponding data reduction, see Ning & Elgered (2021) and Elgered & Ning (2023).

3 Results

The system temperatures, at the three elevation angles, are shown in Fig. 6. The larger scatter in February–March with OW is expected, given the higher system temperatures of that receiver (see Fig. 5).

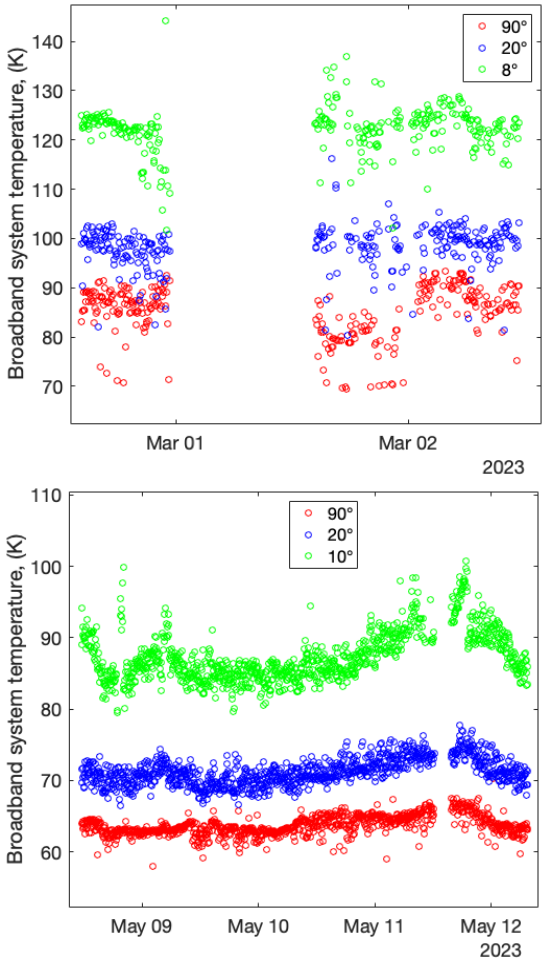

Fig. 6 Average system temperature over 1 min and over the 16 frequency bands (both polarizations) from February–March (OW top) and May (OE bottom).

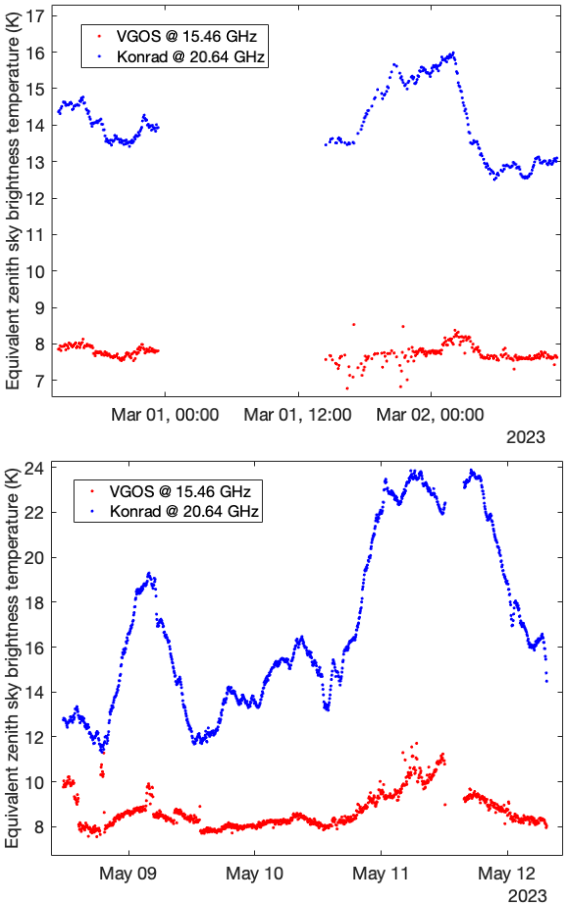

Fig. 7 Equivalent zenith sky brightness temperatures, (February-–March (OW top) and May (OE bottom).

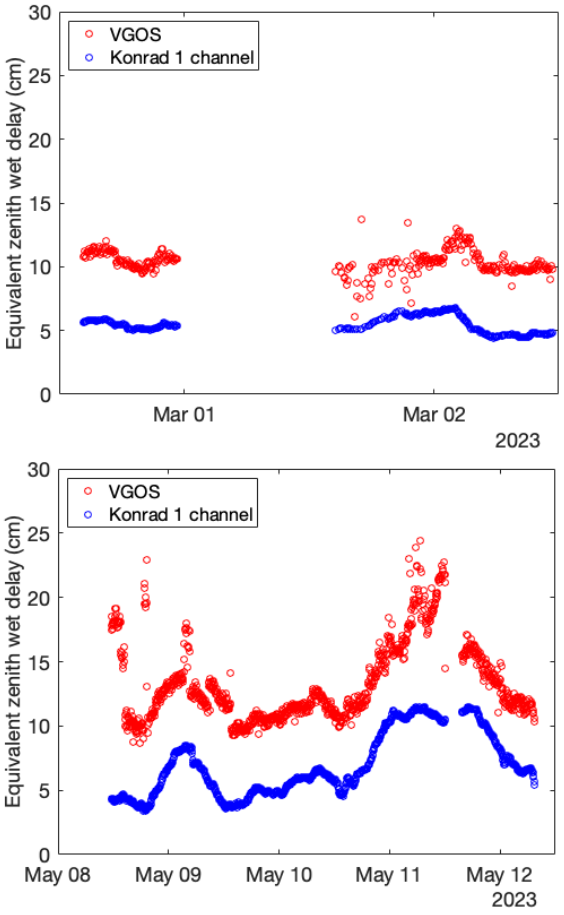

Fig. 8 Equivalent zenith wet delays, February–March (OW top) and May (OE bottom).

The equivalent zenith sky brightness temperatures are shown in Fig. 7 together with the zenith brightness temperatures from the Konrad WVR. These graphs clearly illustrate the lower sensitivity for water vapour at a frequency of 15.46 GHz and, therefore, there is a demand for a very high accuracy of the estimated sky brightness temperatures from VGOS. For the Konrad WVR channel at 20.64 GHz, an error of 1 K in the zenith sky brightness temperature corresponds to an error in the ZWD of 0.6 cm, whereas a 1 K error at the VGOS centre frequency of 15.46 GHz corresponds to a ZWD error of 5.4 cm.

The equivalent ZWD from Konrad, the stand-alone WVR, and estimates from the VGOS receivers are presented in Fig. 8. They were obtained as described by Forkman et al. (2021). Table 1 summarizes the ZWD comparison. Statistics are shown for the two complete sessions and for one selected period from each session when the VGOS receivers were more stable. We immediately notice a very large bias, of the order of 5 cm for both experiments. We speculate that there are two obvious causes.

The first being an increased ground noise pick up by VGOS with a decreasing elevation angle. No model for the ground-noise pickup was applied in our analysis. Due to the high demand on accuracy, 0.1 K or better, such a model will be difficult to produce given that the emission from the ground is not constant as a function of time and azimuth angle.

The second possible cause is an error in the absolute value of the equivalent noise temperature inserted by the noise diode. Because the 15 GHz frequencies are normally not used in VGOS experiments we carried out a quick calibration of the noise diode us-

Table 1 ZWD comparison VGOS radiometry – Konrad WVR

Time period	Bias (cm)	SD (cm)	Correlation coefficient
28 Feb–2 Mar (OW)	4.9	0.9	0.42
28 Feb (OW)	5.2	0.4	0.84
8–12 May (OE)	6.3	2.1	0.73
10–12 May (OE)	5.9	1.6	0.87

ing CasA as the calibration source. Assuming an uncertainty of 10 % in the noise-diode output we find that this introduces an error in the equivalent zenith sky brightness temperature of 0.5 K. This corresponds to a ZWD error of 2.7 cm.

Together these error sources could explain a bias of 5 cm in the ZWD. The effect due to ground-noise pickup could be reduced significantly if the tip-curve method based on the least square fit was not carried out. Instead one could use the individual observations of the brightness temperatures without any averaging. For these frequencies that would, however, pose unrealistic demands on the accuracy of the receiver temperature and the equivalent temperature inserted by the noise diode.

When the biases are removed we observe standard deviations (SD) of the differences of the order of 0.4 cm for a selected period in February when the atmosphere was stable, and 1.6 cm for a more variable period in May. This is roughly in agreement with the simulations in Fig. 2. It is clear that the accuracy of wet delay estimates from geodetic analysis of VLBI observations is usually much higher. Formal errors of less than 2 mm have been reported, e.g. by Elgered et al. (2019), from the analysis of legacy S/X experiments.

4 Conclusions and outlook

We conclude that even a frequency as low as 15 GHz can provide radiometric information about the wet delay, but it requires a careful screening of the data for receiver instabilities and interferences.

Nevertheless, observations at 15 GHz are too far away from the water vapour emission line in order to be useful for an assessment of the ZWD estimates from standard VGOS geodetic processing. The quality (uncertainty) of the estimated ZWD from a geodetic analysis pf S/X legacy VLBI data is less than 2 mm (formal error) (Elgered et al., 2019). The ZWD uncertainty from a geodetic analysis of VGOS data will be even lower, given the increased number of observations compared to legacy S/X. This uncertainty is significantly lower than our observed standard deviations obtained when comparing the ZWD from VGOS radiometry to those from the stand-alone WVR Konrad.

Future VGOS radiometry at frequencies closer to the water vapour emission line at 22.2 GHz will still require improvements in the stability and the calibration of the noise diode and hence the receiver noise temperature. Furthermore, the ground-noise pickup shall be investigated in detail, possibly resulting in a model for the corrections needed.

References

Balanis C A (2005). *Antenna Theory: Analysis and Design (3rd ed.)*, Chap. 2, John Wiley & Sons, New York, p. 34.

Elgered G, Ning T, Forkman P, & Haas R (2019) On the information content in linear horizontal delay gradients estimated from space geodesy observations *Atmos. Meas. Tech.*, 12, 3805–3823, https://doi.org/10.5194/amt-12-3805-2019.

Elgered G & Ning T (2023) On the use of water vapour radiometry for assessment of wet delay estimates from space geodetic techniques, *these proceedings*.

Forkman P, Flygare J, & Elgered G (2021). Water vapour radiometry in geodetic very long baseline interferometry telescopes: assessed through simulations, *J. Geodesy*, 95:117, https://doi.org/10.1007/s00190-021-01571z

Ning T, & Elgered G (2021) High-temporal-resolution wet delay gradients estimated from multi-GNSS and microwave radiometer observations *Atmos. Meas. Tech.*, 14, 5593–5605, https://doi.org/10.5194/amt-14-5593-2021.

Pantaleev M, Helldner L, Haas R, et al. (2017). Design, implementation and tests of the signal chain for the twin telescopes at Onsala Space Observatory, *Proc. of the 23rd European VLBI Group for Geodesy and Astrometry Working Meeting*, eds. R Haas and G Elgered, Gothenburg, 15–19.

Petrachenko B, Niell A, Behrend D, et al. (2009). Design aspects of the VLBI2010 system. In: *Progress report of the IVS VLBI2010 committee*, NASA/TM-2009-214180.

Wu S C (1979). Optimum frequencies of a passive microwave radiometer for tropospheric path-length correction, *IEEE Trans. Ant. Propagat., AP-27, 233–239, https://doi.org/10.1109/TAP.1979.1142066.*